

## All-electron local-density theory of the rippled NiAl(110) surface

J. I. Lee,\* C. L. Fu, and A. J. Freeman

*Department of Physics and Astronomy, Northwestern University, Evanston, Illinois 60201*

(Received 17 June 1987; revised manuscript received 17 September 1987)

The structural and electronic properties of the rippled NiAl(110) surface are investigated using the all-electron total-energy local-density full-potential linearized augmented-plane-wave method. Surface states are found to have  $\approx 1.3$ -eV binding energies at  $\bar{\Gamma}$ — in excellent agreement with the Auger spectra data. The geometry of the rippled surface and the optical-phonon frequency at  $\bar{\Gamma}$  are determined by means of frozen phonon calculations. In good agreement with recent experiments, we find the rippling to be 0.20 Å for the composite Ni-Al surface layer with Al displaced outwards relative to the contracted Ni layer. A possible mechanism behind the surface rippling is discussed in terms of charge-transfer effects and electrostatic neutrality. The charge densities and calculated work functions for the relaxed and unrelaxed surfaces are also reported and discussed in relation to this mechanism.

Recent experiments on NiAl(110)<sup>1,2</sup> and Ni<sub>3</sub>Al(110)<sup>3</sup> have revealed rippled surface relaxation for these alloy surfaces. From their LEED analysis on NiAl(110), Davis and Noonan<sup>1</sup> have shown that the top composite Ni-Al layer possesses a large rippled relaxation with the Al site being displaced approximately 0.22 Å above the Ni site [c.f. Fig. 1(a)]; subsequently, Yalisove and Graham<sup>2</sup> obtained similar results by use of the medium-energy ion scattering method. These interesting observations have generated wide interest and have stimulated theoretical and computational investigations.<sup>4-11</sup> Early theoretical attempts to investigate surface relaxation were limited to the semiempirical potential method,<sup>4</sup> tight-binding approximation,<sup>5,6</sup> or to simplified model Hamiltonians.<sup>7,8</sup> These approaches were not able to describe precisely the delicate energetics or to reveal the detailed features of the driving mechanism behind surface relaxation phenomena. More recently, Chen, Voter, and Srolovitz<sup>9</sup> simulated the relaxation at various Ni-Al alloy surfaces including NiAl(110) by the embedded-atom method;<sup>12</sup> they presented the surface structure of NiAl(110), but were not concerned about the electronic structure and the mechanism behind the rippled relaxation. It is thus desirable to investigate the electronic and structural properties of NiAl(110) by precise band method and to obtain an accurate description of the mechanism behind the surface rippling based on detailed information about the electronic structure. Highly precise first-principles band methods, based on the local-density functional formalism,<sup>13</sup> are presently available for the detailed description of surface relaxation effects—as demonstrated in recent calculations—such as multilayer relaxation for the W(100)<sup>14</sup> and Al(110)<sup>15</sup> surfaces.

The purposes of the present study<sup>10</sup> are (1) to determine the rippled surface geometry and to understand the mechanism behind the surface rippling, and (2) to investigate the surface electronic properties such as the charge density, work function, and surface states, etc., of the NiAl(110) surface. Our highly precise all-electron total-energy study shows that the surface Ni atoms are con-

tracted into the bulk region by  $(8.0 \pm 0.5)\%$  and that the Al atoms expand out to vacuum region by  $(1.5 \pm 0.5)\%$  relative to the unrelaxed interlayer spacing (for a total surface rippling of 0.20 Å). These results are in fairly good agreement with the experimental data from LEED<sup>1</sup> and ion scattering.<sup>2</sup> The surface states are found to have a binding energy of  $\approx 1.3$  eV at  $\bar{\Gamma}$ . We also predict that the work function is 5.17 eV and the optical phonon frequency at  $\bar{\Gamma}$  is 28.5 meV. The mechanism behind the rippled relaxation can possibly be attributed to the charge transfer which serves to maintain the electrostatic neutrality for each layer.

In this investigation, the NiAl(110) surface is represented by a single slab consisting of five atomic layers. To find out the rippled surface geometry, the total energies are calculated for various Ni and Al atomic positions at the surface layer by the full-potential linearized augmented-plane-wave (FLAPW) method.<sup>16,17</sup> The Kohn-Sham local-density functional (LDF) equations incorporating the Hedin-Lundqvist exchange-correlation potential<sup>18</sup> are solved self-consistently for each trial geometry. A total of  $2 \times 360$  LAPW basis functions are used to expand the wave functions. In all the calculations, the muffin-tin radii of Ni and Al spheres are set to the same value, 2.215 a.u. The unrelaxed interlayer spacing corresponds to one-half of the experimental lattice constant, 7.7001 a.u. (also employed in our calculation). Charge densities inside the muffin-tin spheres are expanded in lattice harmonics with angular momentum up to  $l=8$ . The core electrons, including the  $3p$  states of Ni, are treated fully relativistically and the valence electrons derived from the atomic  $3d, 4s$ , and  $4p$  orbitals are treated semirelativistically,<sup>19</sup> i.e., dropping the spin-orbit term, but keeping the other relativistic terms in the Hamiltonian. Up to 32  $k$  points in the irreducible wedge of the two-dimensional (2D) rectangular Brillouin zone are used for the Brillouin-zone integration and a Gaussian broadening scheme is employed). Self-consistency is assumed when the root-mean-square difference of the input and output charge densities is less than  $5 \times 10^{-4}$

electrons/(a.u.)<sup>3</sup>; by then the total energy is stable to within 0.2 mRy.

The total energies were calculated for nine trial geometries and then least-squares fitted by parabolic polynomials in the 2D variational space to determine the stable geometry and optical-phonon frequency at  $\bar{\Gamma}$ . The rippled surface corresponding to the total-energy minimum is for Ni atoms contracted into the bulk region by  $(8.0 \pm 0.5)\%$  [in percentage, relative to  $d_{12}$ , the unrelaxed (110) interlayer spacing], and Al atoms moved outwards by  $1.5 \pm 0.5\%$  from their bulk truncated positions. Although these calculated values of atomic displacement are different from those obtained from LEED ( $-6\%$  for Ni and  $4.6\%$  for Al), the trend of the relaxation is consistent. Perhaps more significantly, the magnitude of the surface rippling ( $0.20 \text{ \AA}$ ) is in excellent agreement with the LEED analysis ( $0.22 \text{ \AA}$ ). A similar value for the surface rippling was recently obtained by the self-consistent pseudopotential method.<sup>11</sup>

Recently, a very similar result for the surface rippling was obtained by ion scattering.<sup>2</sup> Further, this experiment also demonstrated that the amount of subsurface rippling is relatively small compared with that of the surface layer (the subsurface Ni and Al atomic positions are relaxed by about  $1\%$  with a  $180^\circ$  phase difference from those of the corresponding surface atomic displacements). Motivated by this observation, we have carried out a calculation with the subsurface atomic positions given by the results of ion scattering and with the surface atoms at their calculated rippled position. The resultant total energy obtained by allowing the second-layer relaxation is lower than that for an unrelaxed second layer. (The difference is very small, however—only 5 meV.) This result is thus consistent with the small amount of subsurface rippling expected from the short-ranged metallic screening. (Although the energy minimization was not carried out by simultaneously varying both the surface and subsurface atomic positions, the subsurface Ni and Al equilibrium positions should be very close to those of the bulk truncated posi-

tions as shown by the small total-energy difference stated above.)

The optical-phonon frequency at the  $\bar{\Gamma}$  point, for vibrations normal to the surface plane, was estimated to be  $\omega = 28.5 \text{ meV}$  from the curvature of the total-energy minimum path about its relaxed position.

Having established the geometry of the rippled NiAl(110) surface, we now consider the mechanism behind the surface rippling. For this purpose we show in Fig. 1, the charge-density contour plots on the plane (112). [Note that the nearest neighbors to surface Ni(Al) atoms are two subsurface Al (Ni) atoms]. As the surface is created, there is a "spill-out" charge ( $\approx 0.2 \text{ e/unit cell}$ ) into the vacuum region due to the reduced coordination for the surface atoms. This spill-out charge is  $s, p$ -like and acts to screen the discontinuity caused by the formation of the surface. As a result, despite the ionicity of NiAl, the electron charge density in the vacuum region shows a smooth and structureless distribution (i.e., only a small corrugation). In contrast, a quite different charge distribution is seen in the interstitial region just one layer beneath the surface layer [cf. Fig. 1(a)], where the charge density is bulklike and reflects the ionicity of the NiAl alloy. Further, due to the extended nature of the Al  $s, p$  electrons, there is a large amount of interstitial electronic charge distributed beneath the surface Ni sites. Therefore, a strong surface dipole field acting along the surface normal (with the negative end pointing into the surface) is formed on the surface Ni site for the unrelaxed surface. The corresponding electrostatic field on the Al site arising from the dipole charge distribution is considerably smaller, due to the localized nature of the Ni  $d$  electrons and the lower amount of  $s, p$ -like electrons for Ni atoms (recall that the nearest neighbors to surface Al atoms are subsurface Ni atoms). Consequently, in order to maintain electrostatic neutrality, the positive ion cores in the surface layer should move to their individual electrostatic center, i.e., a large inward contraction (into the bulk region) for Ni and a relatively small relaxation for

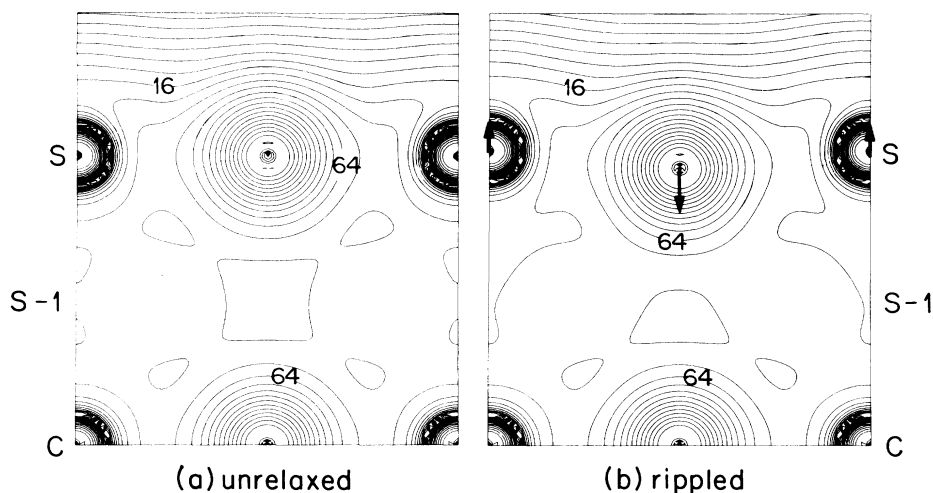


FIG. 1. Valence electronic charge-density contour plots for (a) the unrelaxed and (b) the rippled NiAl(110) surface geometries (with  $\Delta_{\text{Al}}: +4\%$ ,  $\Delta_{\text{Ni}}: -8\%$ ) on the (112) plane. Subsequent contour lines differ by a factor of  $\sqrt{2}$  and the density contours are shown in units of  $10^{-4} \text{ e/(a.u.)}^3$ .

Al (a small outward expansion).

Meanwhile, the response of surrounding electrons to the atomic displacements is to counterpolarize the force caused by the dipole fields [cf. Fig. 1(b)]: a decrease of interstitial charge beneath the surface Ni sites accompanied by an increased density in/above the surface Ni atoms (the opposite charge redistribution is found for the surface Al sites). Because of this charge-transfer effect, the corrugation of the charge density above the surface layer is even smaller than that for the unrelaxed surface; i.e., the relaxation has the effect of smoothing out the surface roughness by a spatial redistribution of the electronic charge. Further, due to the combination of counterpolarization and charge smoothing effects, the electronic density above the subsurface Ni (Al) sites tends to be increased (decreased) which, in turn, induces nonvanishing dipole forces acting on the subsurface atoms. Consequently, the response of the subsurface atomic relaxations is expected to have a  $180^\circ$  phase difference with respect to that of the surface layer. (However, the magnitude of the subsurface layer relaxation is far less than that of the surface layer relaxation as a result of a less pronounced dipole field.) This picture is clearly consistent with the subsurface relaxation discussed above.

We now consider the surface properties which are correlated with the above electrostatic model (cf. Table I): (1) the calculated work function decreases from 5.31 eV for the unrelaxed surface to 5.18 eV for the rippled surface due to the lowering of the surface dipole barrier (i.e., counterpolarization) as the Ni surface atoms are contracted into the bulk region (although the amount of lowering is partially compensated for by the outward relaxation of surface Al atoms), and (2) the number of electrons within the surface Ni (Al) muffin-tin spheres in-

TABLE I. Angular momentum ( $l$ ) decomposed electronic valence charges in the muffin-tin sphere of a five-layer NiAl(110) film for the unrelaxed and relaxed geometries.  $\Delta_l$  denotes the percentage change of the interlayer spacing between surface and subsurface layers.

	$s$	$p$	$d$	Total
$\Delta_{Al}=0, \Delta_{Ni}=0$				
S	Ni: 0.36	0.28	8.27	8.92
	Al: 0.59	0.57	0.09	1.27
S-1	Ni: 0.39	0.36	8.31	9.06
	Al: 0.55	0.65	0.14	1.36
C	Ni: 0.38	0.36	8.32	9.06
	Al: 0.56	0.65	0.14	1.36
$\Delta_{Al}=4, \Delta_{Ni}=-8$				
S	Ni: 0.38	0.31	8.23	8.98
	Al: 0.59	0.55	0.09	1.24
S-1	Ni: 0.38	0.35	8.30	9.04
	Al: 0.56	0.66	0.15	1.40
C	Ni: 0.38	0.36	8.32	9.06
	Al: 0.56	0.65	0.14	1.36

creases (decreases) as the surface layer is relaxed; and the decreased (increased) interstitial electronic density beneath the surface Ni(Al) sites causes the electrons to become more localized (delocalized) within the muffin-tin spheres of subsurface Al(Ni) sites (cf. Table I). The electrostatic model for the surface relaxation is, in fact, quite general. An asymmetric electron charge distribution at cleaved metallic surfaces was found to be responsible for the surface relaxation in a heuristic model proposed by

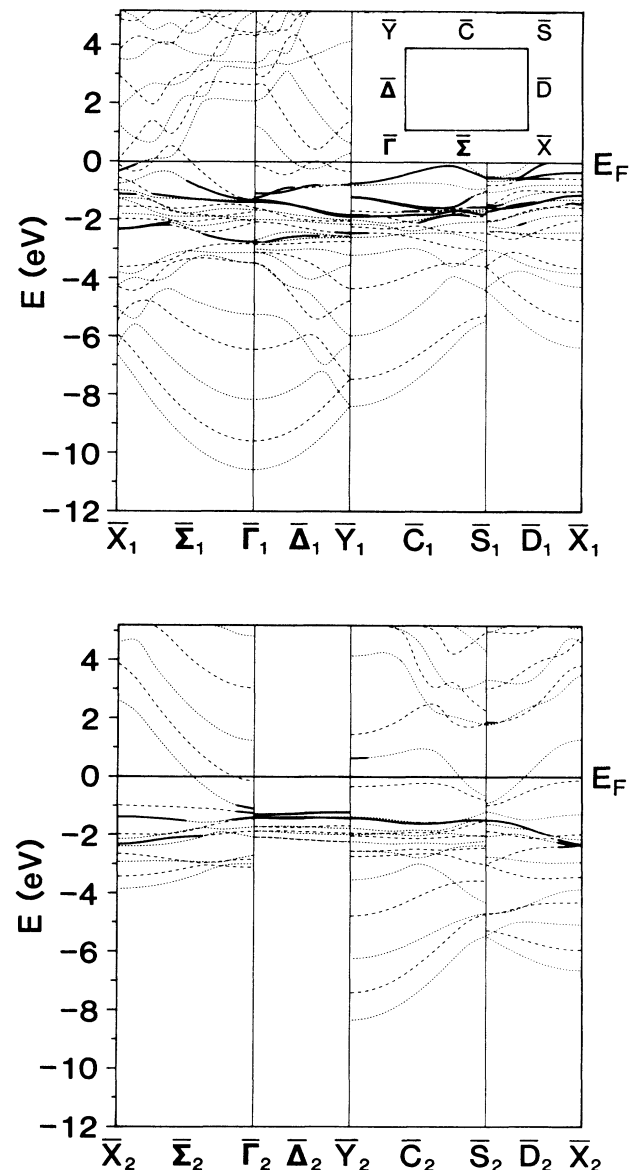


FIG. 2. Energy bands for the rippled [as in Fig. 1(b)] NiAl(110) surface along the high-symmetry directions in the 2D rectangular Brillouin zone as shown in the insert of upper panel. Upper and lower panels show odd and even symmetries with respect to the 2D rotation, respectively. Dashed and dotted lines represent even and odd parities with respect to the  $z$  reflection. Solid lines indicate surface states whose wave functions have more than 50% weight within the surface layer.

Finnis and Heine<sup>20</sup> following the earlier discussion of Smoluchowski<sup>21</sup> about the effect of charge smoothing at metallic surfaces. A similar picture has been applied to the multilayer relaxation on Al(110).<sup>15</sup> The dependence on the bonding character of the electron distribution is considered to be a secondary effect. The large surface rippling for NiAl(110) is simply a manifestation of the charge transfer (ionicity) of NiAl.

We now consider the single-particle energy spectra of the rippled surface as depicted in Fig. 2. The energy bands are plotted along the high-symmetry lines of the 2D rectangular Brillouin zone [shown as inset to Fig. 2(a)]. The energy bands are sorted out for clarity into states with even (upper panel) and odd (lower panel) parities with respect to the 2D rotational symmetry. The dashed and dotted lines represent the states with even and odd parities with respect to  $z$  reflection, respectively. Surface states, denoted by solid curves, are defined as having their wave functions localized by more than 50% in the surface layer. As shown, for each symmetry, we find very localized surface states at the  $\bar{\Gamma}$  point with binding energies =

$\sim 1.3$  eV relative to  $E_F$ . Our calculated binding energies of these surface states are in excellent agreement with the Auger spectra results of Plummer,<sup>22</sup> the observed binding energies of surface states for the  $\bar{\Sigma}_1$  and  $\bar{\Sigma}_4$  symmetries are found to be  $-1.1$  and  $-1.3$  eV, respectively. Our calculated surface states reveal, however, differences in binding energies compared with the calculated normal photoemission spectra for the unrelaxed NiAl(110) surface by König, Redinger, Weinberger, and Stocks.<sup>23</sup> They obtained  $-1.4$  and  $-1.6$  eV for the binding energies of surface states with  $\bar{\Sigma}_1$  and  $\bar{\Sigma}_4$  symmetries, respectively. This deviation might originate from several sources: the effect of their neglected surface relaxation, their use of bulk potentials for the surface layer, and a steplike barrier potential at the vacuum-surface interface.

This work was supported by the National Science Foundation (DMR 85-18607) and a grant from its Division for Advanced Scientific Computing at the University of Illinois National Center for Supercomputing Applications.

\*Permanent address: Department of Physics, Inha University, Inchon, Korea.

<sup>1</sup>H. L. Davis and J. R. Noonan, Phys. Rev. Lett. **54**, 566 (1985).

<sup>2</sup>S. M. Yalisove and W. R. Graham, Bull. Am. Phys. Soc. **31**, 325 (1986).

<sup>3</sup>D. Sondericker, F. Jona, V. L. Moruzzi, and P. M. Marcus, Solid State Commun. **53**, 175 (1985); D. Sondericker, F. Jona, and P. M. Marcus, Phys. Rev. B **33**, 900 (1986).

<sup>4</sup>G. Allan and M. Lannoo, Surf. Sci. **40**, 375 (1973).

<sup>5</sup>G. Treglia, M.-C. Desjonqueres, and D. Spanjaard, J. Phys. C **16**, 2407 (1983), and references therein.

<sup>6</sup>P. C. Stephenson and D. W. Bullett, Surf. Sci. **139**, 1 (1984).

<sup>7</sup>U. Landman, R. N. Hill, and M. Mostoller, Phys. Rev. B **21**, 448 (1980), and references therein.

<sup>8</sup>R. Barnett, U. Landman, and C. L. Cleveland, Phys. Rev. B **27**, 6534 (1983); **28**, 1685 (1983).

<sup>9</sup>S. P. Chen, A. F. Voter, and D. J. Srolovitz, Phys. Rev. Lett. **57**, 1308 (1986).

<sup>10</sup>A brief report of this work presented previously by J. I. Lee, C. L. Fu, and A. J. Freeman, Bull. Am. Phys. Soc. **32**, 772 (1987).

<sup>11</sup>M. H. Kang and E. T. Mele, Bull. Am. Phys. Soc. **32**, 477 (1987).

<sup>12</sup>M. S. Daw and M. I. Baskes, Phys. Rev. B **29**, 6443 (1984).

<sup>13</sup>P. Hohenberg and W. Kohn, Phys. Rev. **136**, B864 (1964); W. Kohn and L. J. Sham, *ibid.* **140**, A1133 (1965).

<sup>14</sup>C. L. Fu, S. Ohnishi, E. Wimmer, and A. J. Freeman, Phys. Rev. Lett. **53**, 675 (1984).

<sup>15</sup>K. M. Ho and K. P. Bohnen, Phys. Rev. B **32**, 3446 (1985).

<sup>16</sup>E. Wimmer, H. Krakauer, M. Weinert, and A. J. Freeman, Phys. Rev. B **24**, 864 (1981), and references therein.

<sup>17</sup>M. Weinert, E. Wimmer, and A. J. Freeman, Phys. Rev. B **26**, 4571 (1982).

<sup>18</sup>L. Hedin and B. I. Lundqvist, J. Phys. C **4**, 2064 (1971).

<sup>19</sup>D. D. Koelling and B. N. Harmon, J. Phys. C **10**, 3107 (1977).

<sup>20</sup>M. W. Finnis and V. Heine, J. Phys. F **4**, L37 (1974).

<sup>21</sup>R. Smoluchowski, Phys. Rev. **60**, 661 (1941).

<sup>22</sup>E. W. Plummer, private communication.

<sup>23</sup>U. König, J. Redinger, P. Weinberger, and G. M. Stocks, Phys. Rev. B **35**, 8243 (1987).